The Influence of Proposed Repository Thermal Load on Multiphase Flow and Heat Transfer in the Unsaturated Zone of Yucca Mountain

Yu-Shu Wu, Sumit Mukhopadhyay, Keni Zhang, and G. S. Bodvarsson

Earth Sciences Division
Lawrence Berkeley National Laboratory
1 Cyclotron Road
Berkeley CA 94720 USA
YSWu@lbl.gov

Abstract

This paper investigates the impact of proposed repository thermal-loading on mountain-scale flow and heat transfer in the unsaturated fractured rock of Yucca Mountain, Nevada. In this context, a model has been developed to study the coupled thermal-hydrological (TH) processes at the scale of the entire Yucca Mountain. This mountain-scale TH model implements the current geological framework and hydrogeological conceptual models, and incorporates the latest rock thermal and hydrological properties. The TH model consists of a two-dimensional north-south vertical cross section across the entire unsaturated zone model domain and uses refined meshes near and around the proposed repository block, based on the current repository design, drift layout, thermal loading scenario, and estimated current and future climatic conditions. The model simulations provide insights into thermally affected liquid saturation, gas- and liquid-phase fluxes, and elevated water and rock temperature, which in turn allow modelers to predict the changes in water flux driven by evaporation/condensation processes, and drainage between drifts.

I. INTRODUCTION

In the last decade, the 500–700 m thick Yucca Mountain unsaturated zone (UZ) has been extensively investigated as a potential subsurface repository for storing high-level radioactive waste. While the site characterization has been carried out mostly for analyzing unsaturated flow and tracer transport in ambient conditions [1, 2], nonisothermal flow and transport processes, created by repository heating from radioactive decay, has also motivated many research efforts. One of the objectives of these research efforts is to understand coupled thermal-hydrological (TH) behavior and its impact on the performance of the proposed repository within the UZ. In particular, some progress has been made in mountain-scale TH modeling studies at Yucca Mountain [3, 4, 5].

Characterizing mountain-scale TH processes at Yucca Mountain has posed a tremendous challenge for investigators. For reliable characterization, laboratory and field investigations are needed. Though field thermal tests extending over tens-of-meters and lasting up to a few years have been carried out at Yucca Mountain, field characterization of mountain-scale (extending over a few kilometers and lasting for hundreds of years) TH

processes is not feasible. Numerical modeling provides a (and possibly the only) powerful tool for analyzing and understanding physical processes on the temporal and spatial scales relevant to mountain-scale flow and heat transfer. Note that, apart from mountain-scale models, the need for numerical/quantitative investigation of coupled TH processes has also motivated development of fluid flow and heat transfer models at other scales [6, 7, 8, 9, 10, 3, 4, 5, 11, 12].

Despite the advances made in modeling TH processes within the UZ at Yucca Mountain, many studies have been limited to small spatial- and/or temporal-scale analysis. For these small-scale TH models, the dual-permeability (DKM) approach has mostly been adopted to conceptualize the flow and transport processes. However, for mountain-scale, multidimensional modeling exercises, the effective continuum model (ECM), rather than the more rigorous DKM, has often been used [3, 10]. This choice primarily results from the fact that the ECM poses less numerical difficulty and requires significantly reduced computational intensity compared to the DKM. Despite these difficulties, with the rapid advances in computer hardware as well as computational algorithms, mountain-scale TH models implementing the DKM concept have also been recently produced [4].

In parallel to mountain-scale TH modeling studies over the past few years, progress has also been made in ambient characterization of UZ flow and transport processes. For example, continual field data collection and analysis, as well as modeling studies conducted over the past few years, have updated and enhanced our understanding of how the UZ system works under natural, ambient conditions [13, 14]. As a result, both UZ geological and conceptual models have been updated [13]. In particular, fracture-matrix rock properties and other model parameters have been better estimated and updated (see Section II). In addition, the repository design and drift layout plans have also been revised, which are different from the ones used in previous mountain-scale TH modeling studies [3, 4].

This paper reports recent work to develop a mountain-scale TH model for characterizing the TH processes in the UZ at Yucca Mountain [10]. The model implements the updated UZ hydrogeological conceptual model and incorporates the updated input parameters from the 3-D model calibration [13]. Using the dual-permeability modeling approach [15], the TH model consists of a two-dimensional (2-D) vertical cross section covering the entire UZ model domain in the north-south direction. In particular, the 2-D TH model is used to investigate spatial and temporal perturbation of temperature, matrix and fracture liquid saturation, and percolation fluxes in the mountain caused by proposed repository heating. Distribution of infiltration fluxes at the top of the mountain and the thermal loading at the repository are the two primary factors that primarily control the evolution of TH processes in the mountain. Changes in the infiltration flux resulting from climate changes have been accounted for in this paper by considering a time-dependent net infiltration map with a three-step increase, representing present-day, monsoon, and glacial climates. The repository thermal loading is represented in this study by considering two separate thermal loading scenarios with or without ventilation along repository drifts.

II. HYDROGEOLOGICAL SETTINGS, MODELING APPROACH, AND NUMERICAL MODEL

The geological model used for developing the numerical grid for the 2-D TH model is based on the current geological framework model [16] for Yucca Mountain. In this geological model, the UZ is organized into layered hydrogeologic units, based primarily on the degree of welding [17]. The primary hydrogeologic units in the UZ are the Tiva Canyon welded (TCw), the Paintbrush nonwelded (PTn), the Topopah Spring welded (TSw), the Calico Hills nonwelded (CHn), and the Crater Flat undifferentiated (CFu).

Shown in Figure 1 is the numerical grid for the mountain-scale 2-D TH model [13], in which the 2-D cross section is represented using an irregular, unstructured, control-volume grid [18]. The 2-D TH model grid (Figure 1) uses refined grid resolution around the repository, and the grid is coarser away from the emplacement tunnels. The 2-D grid has a total of 39,000 gridblocks and 99,000 connections between the gridblocks in a DKM mesh.

The modeling approach in this paper for multiphase flow and heat transfer through fractured rock is based on the DKM method. This approach considers global fluid and heat flow occurring not only between fractures but also between matrix blocks. In such an approach, one rock-volume domain is represented by two separate but interacting continua – one each for the fracture and the matrix. The fracture-matrix fluid flow is evaluated using the quasi-steady-state approximation [19], which has been extended for estimating local energy exchange terms between fracture and matrix systems. [20]. We select the DKM because of its ability to handle flow through both fracture and matrix continua [21, 1].

Simulation of physical processes associated with multiphase flow and heat transfer in fractured rocks of Yucca Mountain are carried out using the TOUGH2 code [22]. Fluid flow and heat-transfer processes in a two-phase, air-water system of fractured rock are described separately using a doublet of governing equations, respectively, for the two continua (fracture and matrix). Two-phase flow is described by the multiphase extension of Darcy's law, whereas relative permeability and capillary functions of both fractures and matrix are assumed to follow the model of van Genuchten [23]. Heat-transfer mechanisms in the two-phase system includes conduction, convection, and radiation, associated with latent heat caused by phase changes in vaporization (boiling) and condensation in the fractured rock. The integral finite-difference scheme is used for spatial discretization, and time discretization is carried out with a backward, first-order, finite-difference scheme. The resulting discrete nonlinear algebraic equations for describing mass and energy conservation are written in a residual form and solved using the Newton/Raphson iteration scheme.

In the mountain-scale TH model, input parameters for fracture and matrix rock are estimated from several previous studies [13, 24, 25]. In addition, thermal properties (such as grain density, wet and dry thermal conductivity, and grain-specific heat) are obtained from [13]. Temperature-dependent fluid properties, such as fluid density, viscosity, and specific enthalpy, are incorporated in the formulation of the TOUGH2 code.

The repository thermal load and its schedule are shown in Figure 2, based on an average initial thermal line load of 1.45 kW/m [26], imposed along each emplacement drift for the radioactive heat source, decreasing with time as a result of radioactive decay. In the actual repository design at Yucca Mountain, approximately 86.3% of the heat during the first 50 years after emplacement of wastes is planned to be removed by ventilation [26]. After the first 50 years, the full thermal load will become applicable. Note that, though the actual process of ventilation is not modeled, the reduced thermal load due to ventilation during the first 50 years has been adopted in the base-case simulations in this paper. The reduced heat load during the first 50 years is also shown in Figure 2. Sensitivity analyses have also been conducted with the mountain-scale TH model with the full thermal load, i.e., no heat is removed by ventilation. These sensitivity studies without ventilation heat removal will be called "no-ventilation" models. Note that the no-ventilation models are not part of the Yucca Mountain repository design.

As shown in Figure 1, the TH model uses the ground surface of Yucca Mountain (or the tuff-alluvium contact in areas of significant alluvial cover) as the top model boundary, and the water table is treated as the bottom model boundary. Both the top and bottom boundaries are specified as constant over time, but spatially varying temperatures and gas pressures. The water table is relatively flat, increasing its elevation only in the north. At the southern part of the model domain, the water table is about 730 m above sea level (masl). Gas pressures are estimated as 92 kPa at an elevation of 730 masl. The surface gas pressures are then determined by running the TOUGH2 software to steady state under given temperature, bottom pressure, and surface-infiltration conditions.

To account for variations in atmospheric temperature with surface elevations in the mountain, measured mean surface temperatures are correlated to elevation using a linear equation. Surface temperatures T_s at any elevation Z are then computed as constants, according to the following equation [1]:

$$T_s = T_{ref} - \lambda\left[Z - Z_{ref}\right] \tag{1}$$

where T_{ref} (=18.23^{o}C) is mean surface temperature at reference elevation Z_{ref} (=1,231 m) and λ is the dry adiabatic atmospheric lapse rate at 0.01^{o}C/m. On the other hand, the temperature distributions at the water table are estimated primarily by contouring the temperature data, measured from boreholes at an elevation of 730 masl [27, 28].

At the top boundary, the mountain-scale TH model uses three net infiltration rates as a step function of time for surface-water-recharge boundary conditions. The three averaged net infiltration rates consist of one present-day and two future (monsoon and glacial infiltration, respectively) scenarios, determined by studies of modern and future climates (BSC, 2004b) for their spatial distributions. The actual timing of the three TH-model infiltration rates are shown in Table 1, indicating average values over the model domain for three time periods: present (0 to 600 years), monsoon (600 to 2,000 years), and glacial transition (2,000 years and beyond).

III. RESULTS AND DISCUSSION

While the mountain-scale TH model generates TH results near the proposed repository, it is preferred that results from more refined and small-scale TH models [26,29] be used for prediction of TH evolution near the source of heat. Because of its large spatial domain, and the subsequent need for using coarser grid blocks in the numerical model, the mountain-scale TH model is more relevant for prediction of TH processes far away from the repository. In this section, we thus discuss the evolution of TH processes at various locations in the mountain.

Temperature

The emplacement drifts at Yucca Mountain are to be located in the middle nonlithophysal and lower lithophysal units of the TSw hydrogeologic unit. To illustrate the impact of repository heating on temperature perturbation in the mountain, simulated temperatures along the PTn-TSw interface (approximately 125-150 meters above the emplacement drifts) are shown in Figure 3. Figure 3a shows temperatures at different times along the PTn-TSw interface with the base-case thermal loading (i.e., 86.3% of the thermal load is removed by ventilation during the first 50 years after emplacement of wastes, see Figure 2). At 100 years, temperatures along the PTn-TSw interface are still below 20°C. In other words, temperatures are still ambient, and the impact of heat has not extended up to that location. At 500 years, however, temperatures at that location have started to increase due to heat from the emplaced wastes. Temperatures are predicted to reach a maximum of about 50°C at 2,000 years along the PTn-TSw. After that, temperatures start to decline. By 8,000 years, temperatures at the PTn bottom have steadily cooled to just above 30°C and are predicted to return to ambient conditions soon after this. In other words, the bottom of the PTn experiences a thermal perturbation not more than 30°C above ambient conditions, and the thermal regime is not expected to last any more than 10,000 years.

The impact of ventilation on the evolution of TH processes at the mountain-scale is shown in Figure 3b, where simulated temperatures along the PTn-TSw interface at various times from the no-ventilation model are compared with the base-case results at the same location. In the no-ventilation thermal-loading scenario, a peak temperature of approximately 65°C (compared to 50°C in the base-case) is realized at the PTn-TSw interface and the peak is reached earlier (around 1,000 years) compared to the base-case. Thereafter, the difference in temperatures from the two thermal-loading scenarios continues to decrease, and at 8,000 years there is no noticeable difference in the temperatures predicted by these two scenarios. Stronger heat loading causes about 10 to 15°C (up to 20 °C) higher peak temperature at the bottom of the PTn in the first 1,000 or so years, and the difference between the temperatures continues to decrease thereafter (becoming similar by 8,000 years). Though not shown here, the evolution of temperature 100-150 meters below the repository is qualitatively similar to that above the repository (i.e. at the PTn-TSw interface as shown in Figure 3).

The signature of boiling and subsequent condensation, which results from the creation of a two-phase zone, is the heat-pipe (i.e., a zone of constant temperature over space or time). As an example, Figure 4 shows the distribution of temperature along a vertical

column from the ground surface to the groundwater table. This column is located near the center of the repository with Nevada coordinates 170,630 m (E-W) and 234,103 m (N-S). The emplacement drift is located around 1,063 masl in this column. Temperature gradually increases from the ground surface till the location of the drift, and then declines thereafter towards the water table. This is true at all times, except between 100–1,000 years for the no-ventilation model (Figure 4a), when there is a heat pipe just above the emplacement drift, where the temperature is constant. This zone of constant temperature signifies the presence of two-phase conditions.

For the case with ventilation (i.e., base-case), the temperature along a vertical column is shown at various times in Figure 4b. Compared to Figure 4a, Figure 4b shows a difference of about 40^{o}C in temperature at the repository horizon at 100 years. Also, since no boiling occurs during ventilation, the heat-pipe signature is absent in Figure 4b. Over time, the difference in temperature at any given location between the two thermal loading scenarios decreases and is no more than 2-5^{o}C by 8,000 years–again illustrating that the effect of ventilation is important only during the first few thousand years, and there too, the impact is most observable close to the emplacement drifts. Note again that, because of averaging over larger gridblock sizes, simulated temperatures (with or without ventilation) near the emplacement drifts with the mountain-scale TH model differ from those of the smaller-scale models [29]. For example, boiling near the emplacement drift is observed even with ventilation when more refined, small-scale models are used [29]. On the other hand, as shown in Figure 4b, no boiling is observed in the base-case (i.e., with ventilation) simulations with the mountain-scale TH model. Note that in the TH model the water table is treated as a fixed-temperature boundary and such as approximation may cause some underprediction in temperature rise in the lower unit near the water table in long times after 1,000 years. However, this treatment is shown to have small impact of variations in simulated temperature at the repository level [4].

Liquid Saturation

Boiling of water leads to redistribution of moisture in the rock matrix. Changes in matrix saturation in the mountain with time are illustrated in Figure 5a (for the no-ventilation case), where matrix saturation along a vertical column is shown at various times. Drying is prominent only around the drift. Elsewhere, matrix saturation changes little from ambient condition, the minor changes attributable to an increase in percolation fluxes at later times owing to climate change. In comparison, matrix saturation along the same vertical column for the case with ventilation shows less moisture redistribution in the matrix, as shown in Figure 5b.

IV. SUMMARY AND CONCLUSIONS

This paper describes a mountain-scale TH model and its ability to assess thermal and hydrological changes in response to repository heat release at Yucca Mountain. The TH model numerically simulates the impact of nuclear-waste heat release on the natural hydrogeological system, including a representation of heat-driven processes occurring in the far field. The mountain-scale TH model can predict thermally affected liquid saturation, gas- and liquid-phase fluxes, and water and rock temperature under repository

thermal load and future climates. Mountain-scale TH model results demonstrate that, when heat is removed by ventilation, rock temperatures around the drift barely reach boiling. Since no significant boiling takes place in this thermal loading scenario, changes in matrix and fracture liquid saturation caused by repository heating are limited. On the other hand, sensitivity studies show that considerable boiling takes place in the vicinity of the repository drifts, particularly, if no heat is removed by ventilation. However, even in this case, the zone of above-boiling temperature is restricted within approximately 10 m around the drifts and the mid-pillar does not reach boiling temperature. Overall, the impact of ventilation on the evolution of TH processes at Yucca Mountain is limited in the vicinity of the drifts and during the first few hundred years or so. Elsewhere in the mountain and at other times, the TH conditions for the two thermal loading scenarios are similar.

It is also observed that temperature perturbation is expected to extend about 200 m above and below the drifts. Temperatures in the mountain are expected to return to pre-emplacement conditions well before 10,000 years. Boiling around the emplacement drifts causes drying in the surrounding rock matrix. Outside the drying zone, in the no-ventilation case, there exists a small zone of increased matrix saturation caused by condensation of displaced pore water by boiling. At larger distances from the drifts, virtually no change occurs in matrix saturation resulting from repository thermal load (for either of the thermal-loading scenarios).

ACKNOWLEDGMENTS

This work was supported by the Director, Office of Civilian Radioactive Waste Management, U.S. Department of Energy, through Memorandum Purchase Order EA9013MC5X between Bechtel SAIC Company, LLC, and the Ernest Orlando Lawrence Berkeley National Laboratory (Berkeley Lab). The support is provided to Berkeley Lab through the U.S. Department of Energy Contract No. DE-AC03-76SF00098. Review and comments of Guoxiang Zhang and Dan Hawkes from Berkeley Lab are greatly appreciated.

References

1. Wu, Y.S., Haukwa, C., and Bodvarsson, G.S., A Site-Scale Model for Fluid and Heat Flow in the Unsaturated Zone of Yucca Mountain, Nevada, Journal of Contaminant Hydrology, 38(1-3), pp. 185-215, 1999.
2. Wu, Y. S., Pan, L., Zhang, W., and Bodvarsson, G.S., Characterization of Flow and Transport Processes within the Unsaturated Zone of Yucca Mountain, Nevada, Under Current and Future Climates, Journal of Contaminant Hydrology, 54(3-4), pp. 215-247, 2002.
3. Haukwa, C.B., Wu, Y-S., and Bodvarsson, G.S., Thermal Loading Studies Using the Yucca Mountain Unsaturated Zone Model, Journal of Contaminant Hydrology, 38(1-3), pp. 217-255, 1999.

4. Haukwa, C.B., Wu, Y-S., and Bodvarsson, G.S., Modeling Thermal–Hydrological Response of the Unsaturated Zone at Yucca Mountain, Nevada, to Thermal Load at a Potential Repository, Journal of Contaminant Hydrology, 62-63, pp. 529-552, 2003.
5. Buscheck, T.A., Rosenberg, N.D., Gansemer, J., and Sun, Y., Thermohydrologic Behavior at an Underground Nuclear Waste Repository, Water Resources Research, 38(3), pp. 1-19, 2002.
6. Tsang, Y.W. and Pruess, K., A Study of Thermally Induced Convection near a High-Level Nuclear Waste Repository in Partially Saturated Fractured Tuff, Water Resources Research, 23(10), pp. 1958-1966, 1987.
7. Pruess, K., Wang, J.S.Y., and Tsang, Y.W., On Thermohydrologic Conditions Near High-Level Nuclear Wastes Emplaced in Partially Saturated Fractured Tuff, 1. Simulation Studies with Explicit Consideration of Fracture Effects, Water Resources Research, 26(6), pp. 1235-1248, 1990.
8. Pruess, K., Wang, J.S.Y., and Tsang, Y.W., On Thermohydrologic Conditions Near High-Level Nuclear Wastes Emplaced in Partially Saturated Fractured Tuff, 2. Effective Continuum Approximation, Water Resources Research, 26(6), pp. 1249-1261, 1990.
9. Buscheck, T.A., Nitao, J.J., and Saterlie, S.F., Evaluation of Thermo-Hydrological Performance in Support of the Thermal Loading Systems Study, High Level Radioactive Waste Management, Proceedings of the Fifth Annual International Conference, Las Vegas, Nevada, May 22-26, 1994. 2, pp. 592-610, 1994.
10. Wu, Y. S., Chen, G., and Bodvarsson, G.S., Preliminary Analysis of Effects of Thermal Loading on Gas and Heat Flow within the Framework of LBNL/USGS Site-Scale Model, LBL-37729: UC-814, Lawrence Berkeley National Laboratory, Berkeley, California, 1995.
11. Mukhophadhyay, S. and Tsang, Y.W., Understanding the Anomalous Temperature Data from the Large Block Test at Yucca Mountain, Nevada, Water Resources Research, 38(10), pp. 28-1–28-12, 2002.
12. Mukhophadhyay, S. and Tsang, Y.W., Uncertainties in Coupled Thermal-Hydrological Processes Associated with the Drift Scale Test at Yucca Mountain, Nevada, Journal of Contaminant Hydrology, 62-63, pp. 595-612, 2003
13. Wu, Y.S., G. Lu, K. Zhang, G. Zhang, H.H. Liu, T. Xu, and E.L. Sonnenthal, UZ Flow Models and Submodels, MDL-NBS-HS-000006 REV02 Bechtel SAIC Company, Las Vegas, Nevada, 2004.
14. Wu, Y. S., Lu, G., Zhang, K., and Bodvarsson, G.S., A Mountain-Scale Model for Characterizing Unsaturated flow and Transport in Fractured Tuffs of Yucca Mountain, Vadose Zone Journal, 3, pp. 796-805. 2004
15. Pruess, K., TOUGH2—A General-Purpose Numerical Simulator for Multiphase Fluid and Heat Flow, LBL-29400, Lawrence Berkeley Laboratory, Berkeley, California, 1991.
16. BSC, Geologic Framework Model (GFM2000), MDL-NBS-GS-000002 REV 02, Bechtel SAIC Company, Las Vegas, Nevada 2004.
17. Montazer, P. and Wilson, W.E., Conceptual Hydrologic Model of Flow in the Unsaturated Zone, Yucca Mountain, Nevada, Water-Resources Investigations Report 84-4345, U.S. Geological Survey, Lakewood, Colorado, 1984.

18. Pan, L., Hinds, J., Haukwa, C.B., Wu, Y-S., and Bodvarsson, G.S., WinGridder - An interactive grid generator for TOUGH, Version 1.0 User's Manual, LBNL-42957, Lawrence Berkeley Laboratory, Berkeley, California, 2001.
19. Warren, J.E. and Root, P.J., The Behavior of Naturally Fractured Reservoirs, Society of Petroleum Engineers Journal, 3(3), pp. 245-255, 1963.
20. Pruess, K. and Narasimhan, T.N., A Practical Method for Modeling Fluid and Heat Flow in Fractured Porous Media, Society of Petroleum Engineers Journal, 25(1), pp. 14-26, 1985.
21. Doughty, C., Investigation of Conceptual and Numerical Approaches for Evaluating Moisture, Gas, Chemical, and Heat Transport in Fractured Unsaturated Rock, Journal of Contaminant Hydrology, 38(1-3), pp. 69-106, 1999.
22. Pruess, K., Oldenburg, C., and Moridis, G., TOUGH2 User's Guide, Version 2.0, LBNL-43134, Lawrence Berkeley National Laboratory, Berkeley, California, 1999.
23. van Genuchten, M.T., A Closed-Form Equation for Predicting the Hydraulic Conductivity of Unsaturated Soils, Soil Science Society of America Journal, 44(5), pp. 892-898, 1980.
24. Ghezzehei, T. A. and H. H. Liu, Calibrated Properties Model, MDL-NBS-HS-000003 REV 02, Bechtel SAIC Company, Las Vegas, Nevada, 2004.
25. Pan, L. and Liu, H.H., Analysis of Hydrologic Properties Data, ANL-NBS-HS-000042 REV 00, Bechtel SAIC Company, Las Vegas, Nevada, 2004.
26. Wu, Y.S, Mukhopadhyay, S., Zhang, K., Sonnenthal, E.L., Zhang, G., and Rutqvist, J., Mountain-Scale Coupled Processes (TH/THC/THM) Models, MDL-NBS-HS-000007 REV03, Bechtel SAIC Company, Las Vegas, Nevada, 2005.
27. Sass, J.H., Lachenbruch, A.H., Dudley, W.W., Jr., Priest, S.S., and Munroe, R.J., Temperature, Thermal Conductivity, and Heat Flow Near Yucca Mountain, Nevada: Some Tectonic and Hydrologic Implications, Open-File Report 87-649, U.S. Geological Survey, Denver, Colorado, 1988.
28. Rousseau J. P., Kwicklis, E.M., and Gillies, C. (eds.), Hydrogeology of the unsaturated zone, North Ramp area of the exploratory studies facility, Yucca Mountain, Nevada, U.S. Geological Survey, Water-Resources Investigations 98-4050, 1998.
29. 29. Birkholzer, J.T., Mukhopadhyay, S., and Tsang, Y.W., Drift-Scale Coupled Processes (DST and TH Seepage) Models, MDL-NBS-HS-000015 REV 03, Bechtel SAIC Company, Las Vegas, Nevada, 2005.

Table 1. Averaged infiltration rates (mm/yr) and time period over the 2-D TH model domain [26]

Scenario	**Time Period**	**Mean Infiltration (mm/yr)**
Present-Day/Modern	0–600 Years	5.8
Monsoon	600–2,000 Years	17.0
Glacial Transition	2,000 and beyond	28.8

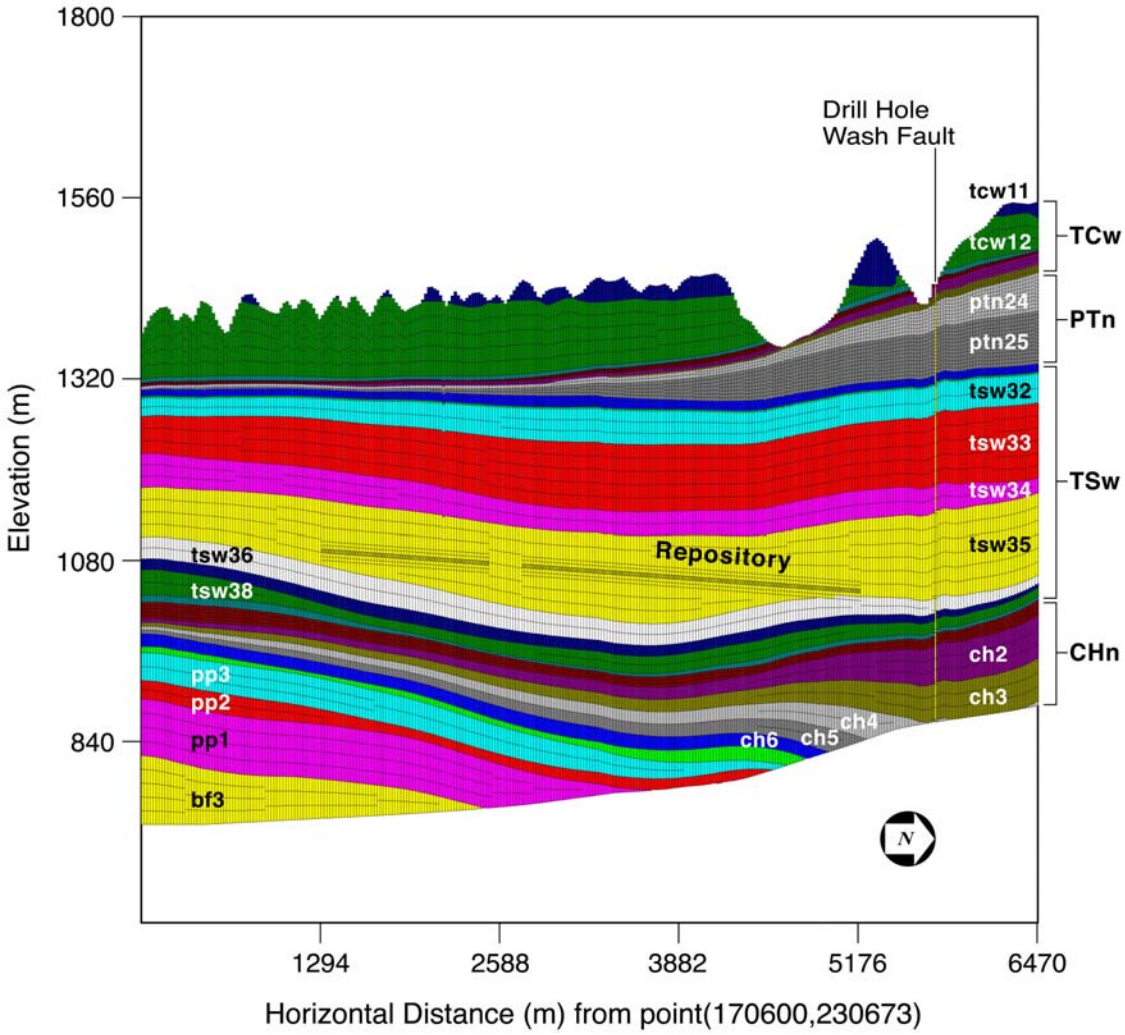

Figure 1. 2-D north-south cross-sectional model domain and grid showing lateral and vertical discretization, hydrogeological layers, repository layout, and a fault

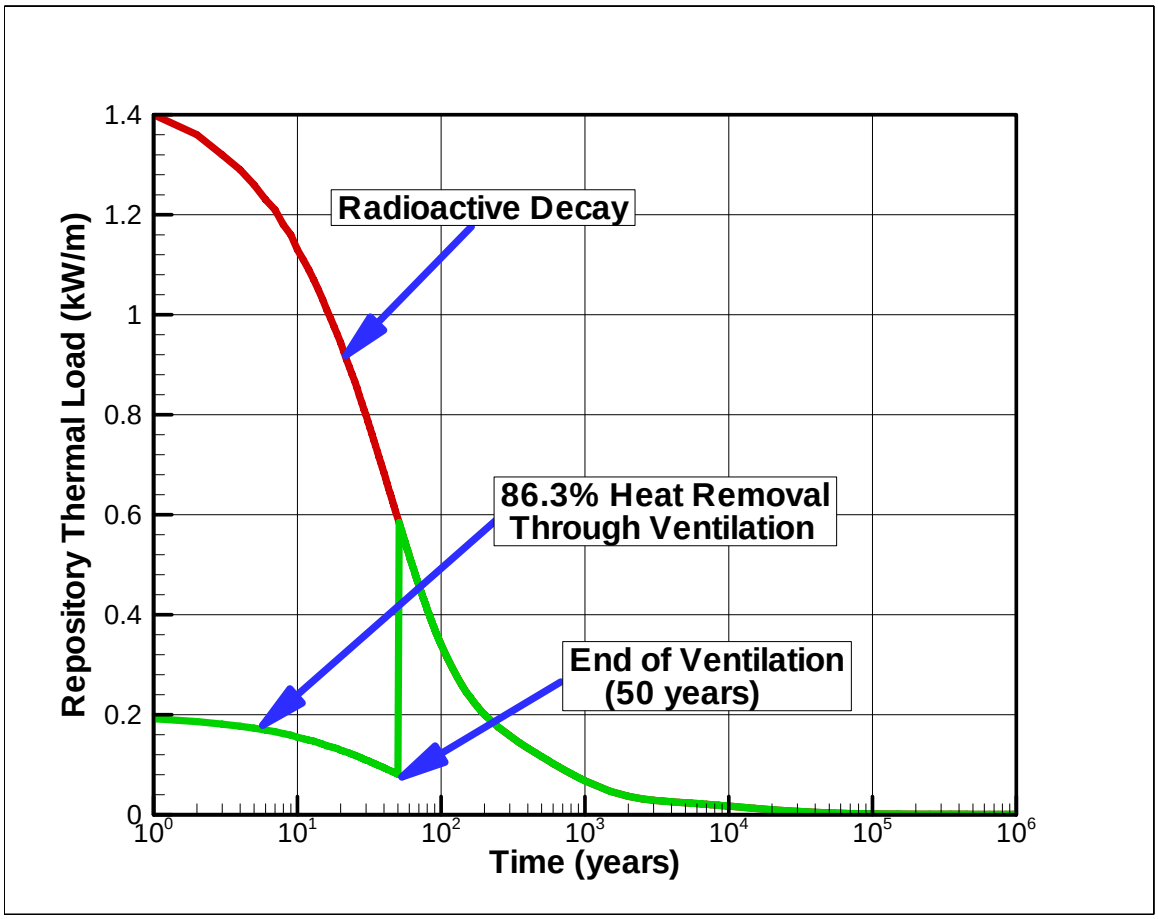

Figure 2. Radioactive heat decay curve for an initial thermal load of 1.45 kW/m. showing the thermal load when 86.3% of the heat is removed by ventilation during the first 50 years [26]

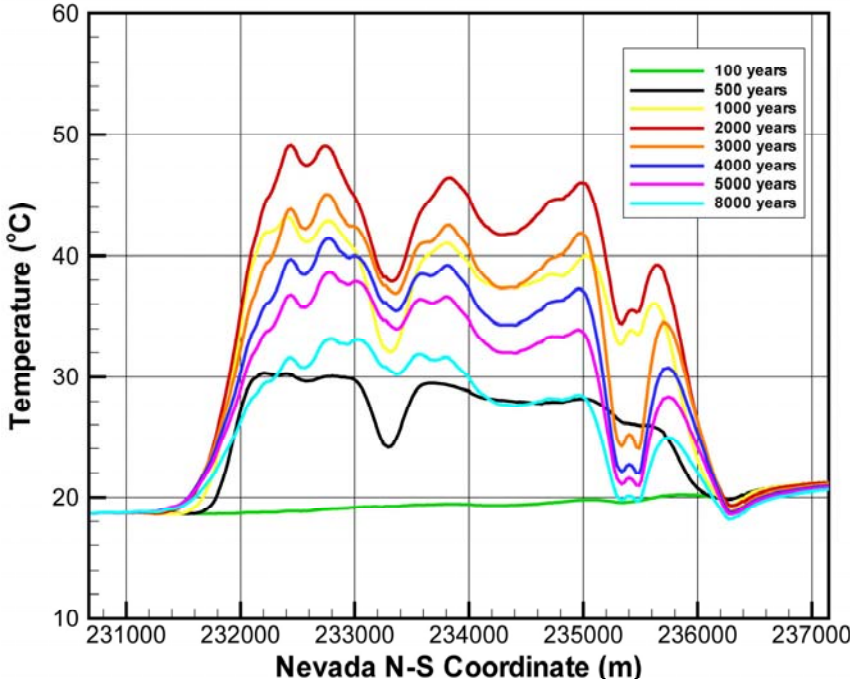

Figure 3a. Simulated rock temperatures along the PTn-TSw interface (~125-150 m above the emplacement drifts) at various times using the bas-case model

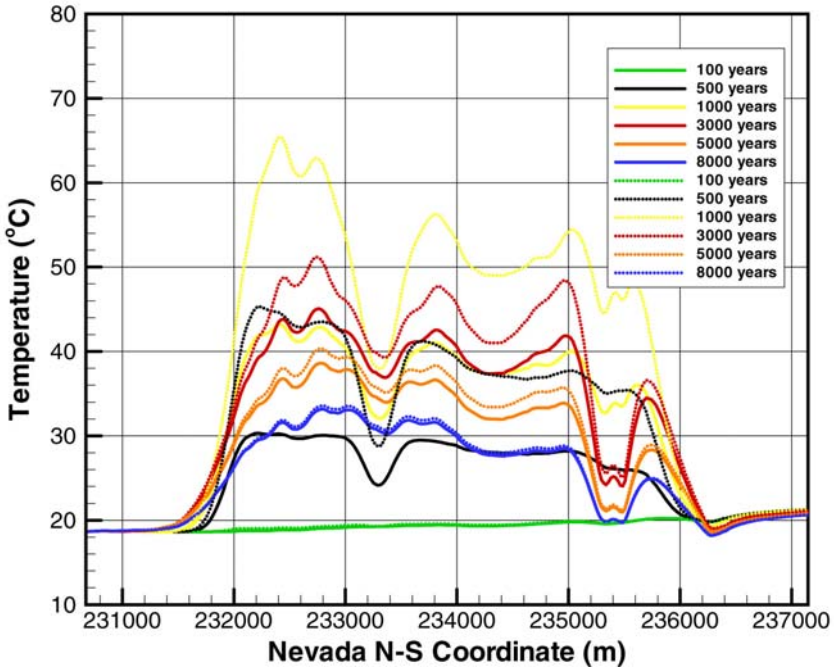

Figure 3b. Comparison of temperature along the PTn-Tsw interface using the base-case (solid lines) and no-ventilation case (dotted lines) models

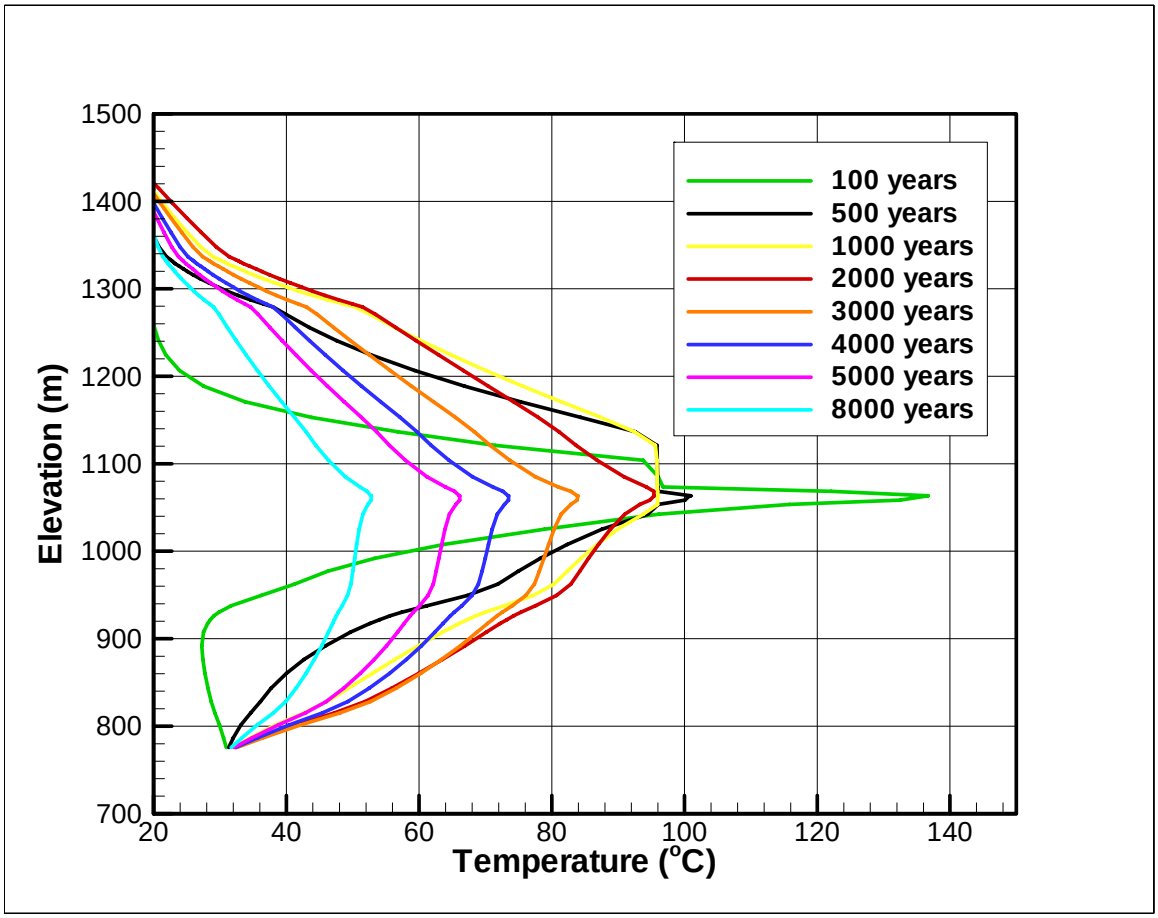

Figure 4a. Simulated rock temperature along a vertical column from the ground surface to water table as with the no-ventilation model

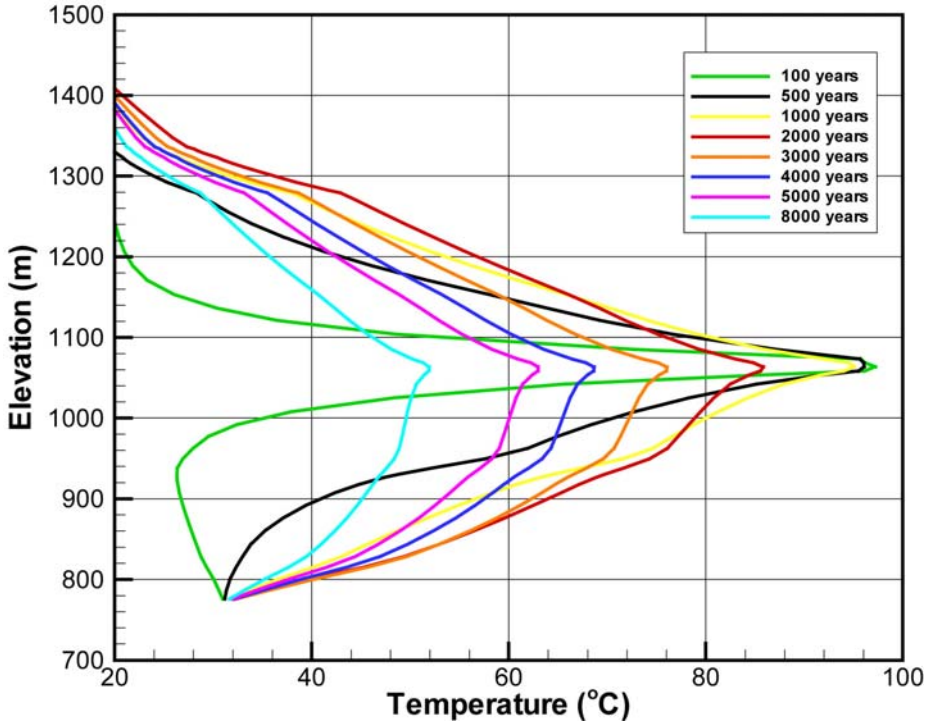

Figure 4b. Simulated rock temperatures with the base-case model. Compare this figure with Figure 4a.

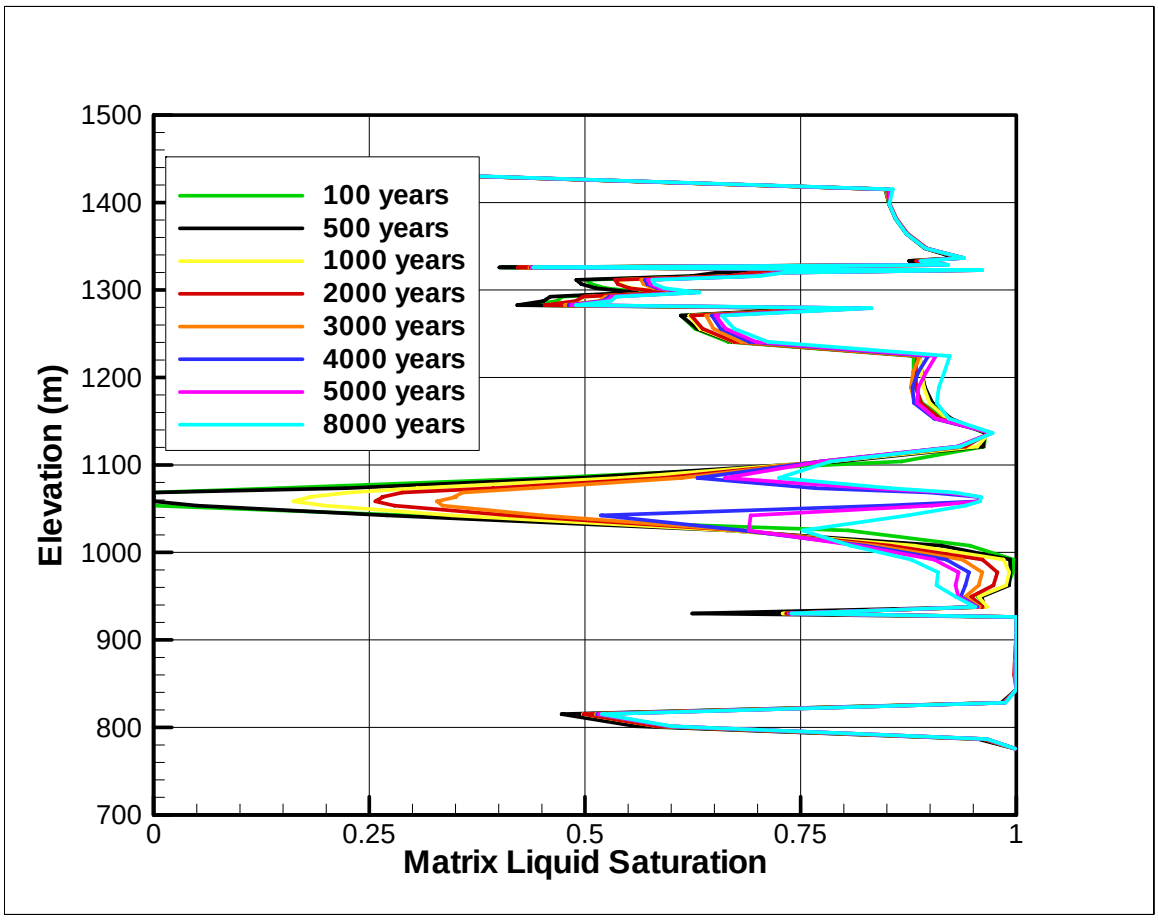

Figure 5a. Simulated matrix saturation along a vertical column from the ground surface to water table as predicted with theno-ventilation model

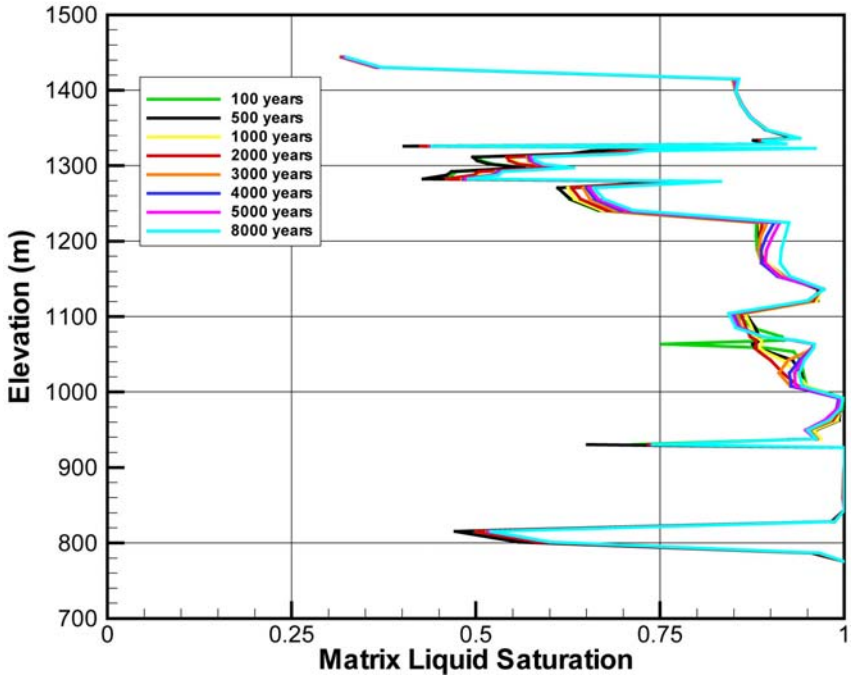

Figure 5b. Simulated matrix saturation along a vertical column as predicted with the base-case model Compare this figure with Figure 5a.